

# Critical Line in Random Threshold Networks with Inhomogeneous Thresholds

Thimo Rohlf

*Santa Fe Institute, 1399 Hyde Park Road, Santa Fe, NM 87501, U.S.A*

(Dated: November 20, 2018)

We calculate analytically the critical connectivity  $K_c$  of Random Threshold Networks (RTN) for homogeneous and inhomogeneous thresholds, and confirm the results by numerical simulations. We find a super-linear increase of  $K_c$  with the (average) absolute threshold  $|h|$ , which approaches  $K_c(|h|) \sim h^2/(2\ln|h|)$  for large  $|h|$ , and show that this asymptotic scaling is universal for RTN with Poissonian distributed connectivity and threshold distributions with a variance that grows slower than  $h^2$ . Interestingly, we find that inhomogeneous distribution of thresholds leads to increased propagation of perturbations for sparsely connected networks, while for densely connected networks damage is reduced; the cross-over point yields a novel, characteristic connectivity  $K_d$ , that has no counterpart in Boolean networks. Last, local correlations between node thresholds and in-degree are introduced. Here, numerical simulations show that even weak (anti-)correlations can lead to a transition from ordered to chaotic dynamics, and vice versa. It is shown that the naive mean-field assumption typical for the annealed approximation leads to false predictions in this case, since correlations between thresholds and out-degree that emerge as a side-effect strongly modify damage propagation behavior.

PACS numbers: 05.45.-a, 05.65.+b, 89.75.-k, 89.75.Da

## I. INTRODUCTION

Many systems in nature, technology and society can be described as complex networks with some flow of matter, energy or information between the entities the system is composed of; examples are neural networks, gene regulatory networks, food webs, power grids and friendship networks. Often, in particular when the networks considered are very large, many details of the topological structure as well as of the dynamical interactions between units are unknown, hence, statistical methods have to be applied to gain insight into the global properties of these systems. In this spirit, Kauffman [1, 2] introduced the notion of Random Boolean Networks (RBN), originally as a simplified model of gene regulatory networks (GRN). In a RBN of size  $N$ , each node  $i$  receives inputs from  $0 \leq k \leq N$  other nodes (with  $k$  usually either considered to be constant, or distributed according to a Poissonian with average  $\bar{K} \ll N$ ), and updates its state according to a Boolean function  $f_i$  of its inputs; the subscript  $i$  indicates that Boolean functions vary from site to site, usually assigned at random to each node. It was shown that RBN exhibit a percolation transition from ordered to chaotic dynamics at a critical connectivity  $\bar{K} = K_c = 2$ . Since interactions in RBN are asymmetric and hence a Hamiltonian does not exist, mean-field techniques have to be applied for analytical calculation of critical points, for example the so-called *annealed approximation* (*annealed approximation*) introduced by Derrida and Pomeau [3, 5, 6]. In the annealed approximation, random perturbations are applied to initial dynamical states, and random ensemble techniques are applied to determine whether the so-induced "damage" spreads over the network or not. Recent research has revealed many surprising details of RBN dynamics at criticality, e.g. super-polynomial scaling of the number

of different dynamical attractors (fixed points or periodic cycles) with  $N$  [7] (while Kauffman assumed it to scale  $\sim \sqrt{N}$  [1]), as well as analytically derived scaling laws for mean attractor periods [8] and for the number of frozen and relevant nodes in RBN [9, 10]. Similarly, it was shown recently that dynamics in finite RBN exhibits considerable deviations from the annealed approximation (that is exact only in the limit  $N \rightarrow \infty$ ) [11, 12]. Boolean network models have been applied successfully to model the dynamics of real biological systems, e.g. the segment polarity network of *Drosophila* [13], dynamics and robustness of the yeast cell cycle network [14], damage spreading in knock-out experiments [15] as well as establishment of position information [16] and cell differentiation [17] in development. Other models explicitly evolve RBN topology according to local rewiring rules coupled to local order parameters of network dynamics (e.g., the local rate of state changes), and investigate the resulting self-organized critical state [18, 19, 20].

A drawback of RBN is the fact that, in spite of their discrete nature (which makes them easy to simulate on the computer in principle), the time needed to compute their dynamics in many instances scales exponential in  $N$  and  $\bar{K}$ , and often large statistical ensembles are needed for unbiased statistics due to the strongly non-ergodic character [21] of RBN dynamics. For this reason, there exists considerable interest in simplified models of RBN dynamics, as, for example, *Random Threshold Networks* (RTN), that constitute a subset of RBN.

In RTN, states of network nodes are updated according to a weighted sum of their inputs plus a threshold  $h$ , while interaction weights take (often discrete and binary) positive or negative values assigned at random. The critical connectivity, calculated by means of the annealed approximation, was found to deviate slightly from RBN [22, 23, 24]; this analysis was extended to RTN dynamics

including stochastic update errors [25]. In particular, it was found that phase transitions in RTN with scale-free topologies [25, 26] substantially differ from both RTN with homogeneous or Poissonian distributed connectivity and scale-free RBN [27]. Further, dynamics in finite RTN with  $k = \text{const.} = 2$  inputs per node recently was found to be surprisingly ordered, including, e.g., globally synchronized oscillations [28]. Other approaches, that apply learning algorithms as well as ensemble techniques, present evidence that information processing of static [29] or time-variant [30] external inputs is optimized at criticality in both RBN and RTN.

In this paper, we extend the theoretical analysis of RTN in a number of respects. First, we calculate the critical connectivity  $K_c$  for arbitrary thresholds  $h \leq 0$ , and generalize this derivation for the first time to inhomogeneously distributed thresholds  $h_i$  that can vary from node to node. This generalization, that introduces an additional level of complexity to RTN dynamics, is motivated by recent observations of strong variations in regulatory dynamics from gene to gene in real GRN, caused by, for example, the frequent occurrence of canalizing functions [21] and the abundance of regulatory RNA in multicellular organisms which strongly influence the expression levels and -patterns of (regulatory) proteins [31]. Using the annealed approximation and additional approximation techniques, we derive a general scaling relationship between critical connectivity  $K_c$  and (average) absolute node threshold  $|h|$ , and show that  $K_c(|h|)$  asymptotically approaches a unique scaling law  $K_c(|h|) \sim h^2/(2 \ln |h|)$  for large  $|h|$ . Evidence is presented that this asymptotic scaling law is universal for RTN with Poissonian distributed connectivity and threshold distributions with a variance that grows slower than  $|h|^2$ . Convergence against this scaling law is rather slow (logarithmic in  $|h|$ ); we show that, for finite  $|h|$ , scaling behavior can be approximated well locally by power laws  $K_c(|h|) \sim |h|^\alpha$  with  $3/2 < \alpha < 2$ .

Further, we establish that damage propagation functions of RTN with homogeneous thresholds  $|h|$  and of RTN with inhomogeneous thresholds with the same *average*  $|\bar{h}| = |h|$  intersect at characteristic connectivities  $K_d(|h|) > K_c(|h|)$ , which implies that for  $\bar{K} < K_d$ , random distribution of thresholds tends to increase damage, while for  $\bar{K} > K_d$ , the opposite holds. Evidence is presented that  $K_d(|h|)$  converges to an asymptotic scaling law  $K_d(|h|) \sim h^2$ . We compare the scaling of  $K_d$  to the corresponding case of random Boolean networks (RBN) with inhomogeneously distributed bias, parameterized in terms of a bias parameter  $1/2 \leq p \leq 1$ . It is shown that  $K_d$  is not defined for RBN in the limit  $p \rightarrow 1$ , which corresponds to  $|h| \rightarrow \infty$  in RTN. Hence,  $K_d$  constitutes a truly novel, not previously known concept, yielding a new characteristic connectivity which is well-defined only for RTN.

Last, we investigate the effect of correlations between thresholds  $h_i$  and in-degree  $k_i$ , while keeping all other network parameters constant. We find that even small

positive correlations can induce a transition from supercritical (chaotic) to subcritical (ordered) dynamics, while anti-correlations have the opposite effect. It is shown that the naive mean-field assumption typical for the annealed approximation leads to false predictions in this case. Even in the simplest case, where only in-degree and (absolute) threshold are correlated, complete information about topology, including the output side, has to enter statistics, and the order of averages becomes important.

## II. RANDOM THRESHOLD NETWORKS

A Random Threshold Network (RTN) consists of  $N$  randomly interconnected binary sites (spins) with states  $\sigma_i = \pm 1$ . For each site  $i$ , its state at time  $t+1$  is a function of the inputs it receives from other spins at time  $t$ :

$$\sigma_i(t+1) = \text{sgn}(f_i(t)) \quad (1)$$

with

$$f_i(t) = \sum_{j=1}^N c_{ij} \sigma_j(t) + h_i, \quad (2)$$

where  $c_{ij}$  are the interaction weights. If  $i$  does not receive signals from  $j$ , one has  $c_{ij} = 0$ , otherwise, interaction weights take discrete values  $c_{ij} = \pm 1$ ,  $+1$  or  $-1$  with equal probability. In the following discussion we assume that the threshold parameter takes integer values  $h_i \leq 0$  [34]. Further, we define  $\text{sgn}(0) = -1$ . [35] The  $N$  network sites are updated *synchronously*. Notice that we depart from the well-studied case  $h_i = \text{const.} = 0$  in two respects:  $h_i$  can take arbitrary values  $h_i \leq 0$ , and it can differ from node to node (inhomogeneous thresholds).

Let us now have a closer look on network topology. Let  $\bar{K}$  be the *average connectivity*, i.e. the average number of inputs (outputs) per site, and let us assume that each interaction weight has equal probability  $p = \bar{K}/N$  to take a non-zero value. Further, let us consider the limit of sparsely connected networks with  $\bar{K} \ll N$ . Under these assumptions, the statistical distribution  $\rho_k$  of in- and out-degrees follows a Poissonian:

$$\rho_k = \frac{\bar{K}^k}{k!} e^{-\bar{K}}. \quad (3)$$

Further, we study the case where in- and out-degree distributions differ: while the out-degree is still distributed according to a Poissonian, the in-degree distribution exhibits a power-law tail, i.e.

$$\rho_{k_{in}} \propto k^{-\gamma} \quad (4)$$

with  $2 \leq \gamma \leq 4$ .

### III. CALCULATING THE CRITICAL LINE

#### A. Uniform threshold $h < 0$

We start with the simplest case and assume that all network sites have identical integer threshold values  $h_i \equiv h \leq 0$ . The case  $h > 0$  is not studied here, as it may lead to the pathological outcome of nodes set to an active state  $\sigma_i = +1$ , though they receive only inhibitory inputs  $c_{ij} < 0$ .

Let us first calculate the probability for damage spreading  $p_s(k)$ , i.e. the probability that a node with  $k$  inputs changes its state, if one of its input states is flipped. A straight-forward extension of the combinatorial analysis carried out in [24] for the special case  $h = 0$  yields

$$p_s(k, |h|) = k^{-1} \cdot 2^{-(k+1)} \cdot \left[ (k + |h| + 1) \cdot \binom{k}{\frac{k+|h|+1}{2}} + (k - |h| + 1) \cdot \binom{k}{\frac{k-|h|+1}{2}} \right] \quad (5)$$

$$= 2^{-(k-1)} \binom{k-1}{\frac{k+|h|-1}{2}} \quad (6)$$

for odd  $k - |h|$  with  $k > |h|$ , and

$$p_s(k, |h|) = k^{-1} \cdot 2^{-(k+1)} \cdot \left[ (k - |h|) \cdot \binom{k}{\frac{k-|h|}{2}} + (k + |h| + 2) \cdot \binom{k}{\frac{k+|h|+2}{2}} \right] \quad (7)$$

$$= 2^{-(k-1)} \binom{k-1}{\frac{k+|h|}{2}} \quad (8)$$

for even  $k - |h|$  with  $k > |h|$  (for a detailed derivation, please refer to appendix A). Notice that Eqs. (6) and (8) are similar, yet not identical to the corresponding relations derived in [25] for RTN with probabilistic time evolution; in particular, for the RTN with *deterministic* dynamics as studied here, the relation  $p_s^{odd}(k) = p_s(k-1)$  holds only for the special case  $|h| = 0$ , whereas for  $|h| > 0$ ,  $p_s(k)$  exhibits an oscillatory behavior (Fig. 1).

If we know the statistical distribution function  $\rho_k$  of the in-degree, the average damage spreading probability then simply follows as [24]

$$\langle p_s \rangle = \sum_{k=|h|}^N \rho_k p_s(k+1, |h|), \quad (9)$$

where  $\langle \cdot \rangle$  indicates the average over the ensemble of all possible network topologies that can be generated according to the degree-distribution  $\rho_k$ . In the case of a Poisson distributed connectivity with average degree  $\bar{K}$ , it follows

$$\langle p_s \rangle(\bar{K}, |h|) = e^{-\bar{K}} \sum_{k=|h|}^N \frac{\bar{K}^k}{k!} p_s(k+1, |h|). \quad (10)$$

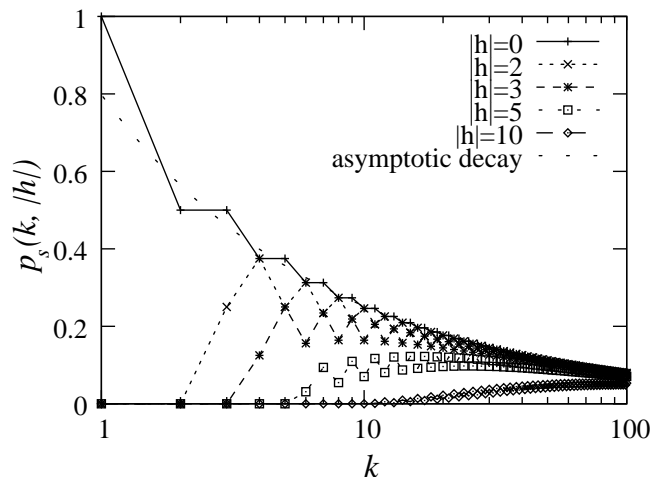


FIG. 1: Probability  $p_s(k, |h|)$  of damage propagation, for different values of the threshold  $|h|$ , as a function of the number of inputs  $k$ . For large  $k$ , the curves asymptotically approach  $p_s \sim 1/\sqrt{k}$  (dashed line). Notice the oscillatory behavior for  $|h| > 0$ .

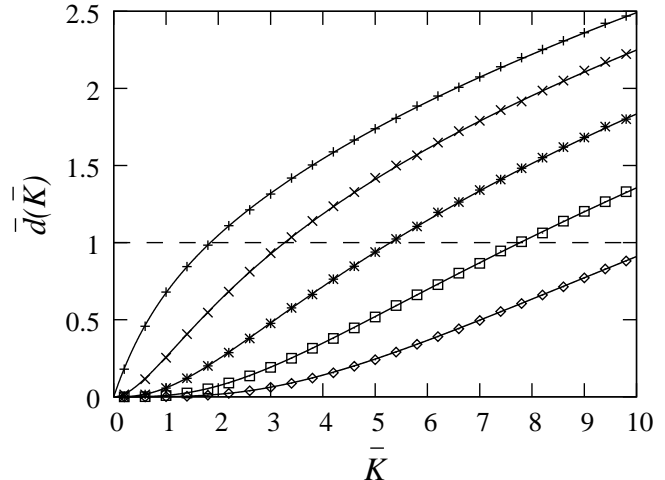


FIG. 2: Expectation value  $\bar{d}$  of damage one time step after a one-bit perturbation, as a function of the average connectivity  $\bar{K}$ , and different (homogeneous) thresholds  $|h|$  ( $|h| = 0$  (+),  $|h| = 1$  (X),  $|h| = 2$  (\*),  $|h| = 3$  (□),  $|h| = 4$  (◇)). Solid curves are the corresponding analytical results obtained from the annealed approximation.

Let us now apply the so-called *annealed approximation* [3], which averages the effect of perturbations over the whole ensemble of possible network topologies *and* all possible state configurations; in this approximation, the expected damage  $\bar{d}$  after one update time step, given a one-bit perturbation at time  $t - 1$  then follows as

$$\bar{d}(t+1) = \langle p_s \rangle(\bar{K}, |h|) \cdot \bar{K}, \quad (11)$$

where  $\bar{\cdot}$  denotes the average over all possible network topologies and all possible state configurations. If we

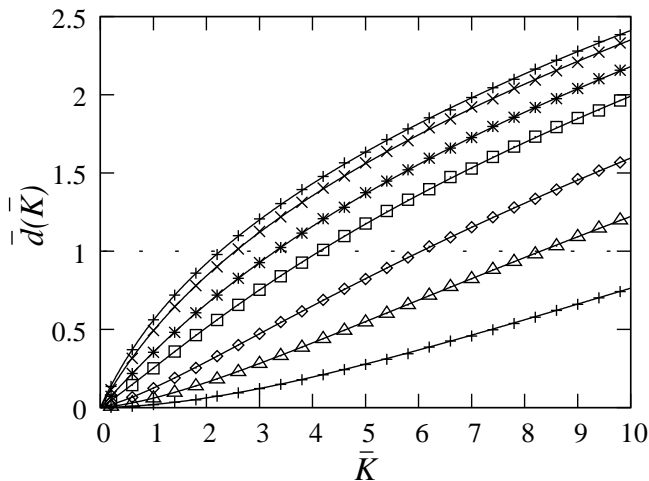


FIG. 3: Average damage  $\bar{d}(\bar{K})$  one time step after a one-bit perturbation, for Poisson-distributed connectivity with average degree  $\bar{K}$ , and Poisson-distributed negative thresholds with average absolute value  $|\bar{h}|$ ; points are data from numerical simulations of RTN (ensemble averages over 100000 different network realizations for each data point), lined curves are analytical solutions (annealed approximation). Numerical data were sampled for  $|\bar{h}| = 0$  (+),  $|\bar{h}| = 0.3$  (X),  $|\bar{h}| = 1.0$  (\*),  $|\bar{h}| = 1.5$  (squares),  $|\bar{h}| = 2.5$  ( $\diamond$ ),  $|\bar{h}| = 3.5$  (triangle) and  $|\bar{h}| = 5.0$  (+).

apply a sufficiently large (but finite) upper limit  $N$  to the sum in Eq. (10), we can numerically evaluate this formula with any desired accuracy. Figure 2 shows the results for the first five values of negative  $h$  of RTN with Poissonian distributed connectivity, compared to measurements obtained from numerical simulations of large ensembles of randomly generated instances of RTN, indicating an excellent match between theory and simulation.

### B. Poisson distributed thresholds

Let us now consider the more general case of non-uniform thresholds, i.e., networks where each site  $i$  has assigned an individual threshold  $h_i \leq 0$ . In the simplest case, we can imagine that the final thresholds resulted from iterated, random decrements (starting from  $h = 0$  for all sites), until a certain average threshold  $\bar{h}$  is reached - this process results in Poisson distributed thresholds  $h_i$ . If threshold assignment is independent from the (also Poisson distributed) in-degree, the probabilities for  $k$  and  $h$  simply multiply, and the resulting average damage propagation probability is

$$\langle p_s \rangle(\bar{K}, |\bar{h}|) = e^{-(\bar{K} + |\bar{h}|)} \sum_{|h|=0}^N \sum_{k=|\bar{h}|}^N \frac{\bar{K}^k |\bar{h}|^{|h|}}{k! |h|!} p_s(k+1, |h|), \quad (12)$$

where  $|\bar{h}|$  is the average absolute threshold.

Figure 3 demonstrates that the expected damage

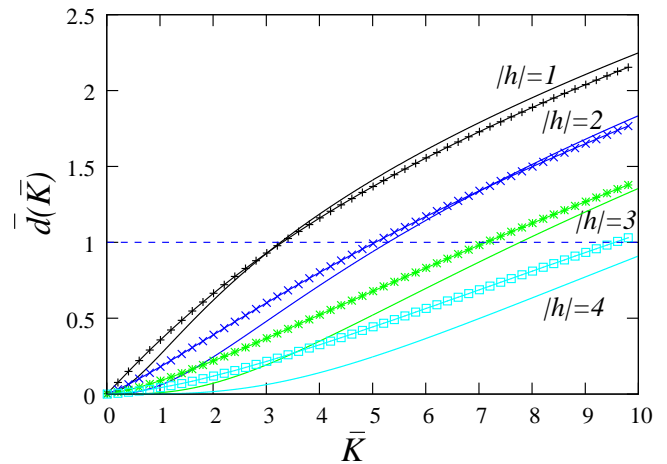


FIG. 4: Comparison of damage spreading in networks with homogeneous thresholds  $|h| = \text{const.}$  (solid lines, threshold values  $|h|$  as indicated) vs. networks with inhomogeneous thresholds distributed according to a Poissonian with the same average threshold  $|\bar{h}|$  (curves with data points,  $|\bar{h}| = 1$  (+),  $|\bar{h}| = 2$  (x),  $|\bar{h}| = 3$  (\*) and  $|\bar{h}| = 4$  ( $\square$ ); results obtained from the annealed approximation).

$\bar{d}_{t+1}(\bar{K}, |\bar{h}|)$  resulting from a one-bit perturbation at time  $t$ , as predicted from this annealed approximation over both degree- and threshold distribution, exhibits excellent agreement with the results obtained from numerical simulations of randomly generated RTN ensembles. It is an interesting question how the dynamics of RTN with inhomogeneous thresholds compares to RTN with homogeneous thresholds. Figure 4 shows  $\bar{d}(\bar{K})$  for RTN with different homogeneous  $|h| = \text{const.}$  and the corresponding inhomogeneous RTN with Poisson-distributed thresholds with the same average  $|\bar{h}| = |h|$ , as obtained from the annealed approximation. One observes that for small  $\bar{K}$ , the curves for RTN with inhomogeneously distributed thresholds are systematically above those of the corresponding homogeneous RTN, i.e., the randomization of node thresholds increases dynamical disorder - also, the critical connectivities  $K_c(|h|)$  (intersections with the line  $\bar{d} = 1$ ) are shifted to smaller values. However, one also realizes that the curves intersect in the super-critical phase at characteristic connectivities  $K_d(|h|)$ , i.e., for  $\bar{K} > K_d(|h|)$ , inhomogeneity in thresholds actually reduces damage.

### C. Universal scaling of the critical line

If we again assume a one-bit perturbation at time  $t$ , the critical line  $K_c(|h|)$ , that separates the ordered and the chaotic phase of RTN dynamics, is given by the condition

$$\bar{d}(t+1) = \langle p_s \rangle(K_c(|h|), |h|) \cdot K_c(|h|) = 1. \quad (13)$$

Again, we can apply Eq. (10) to solve this equation for arbitrary  $h \leq 0$ , however, numerical evaluation is almost

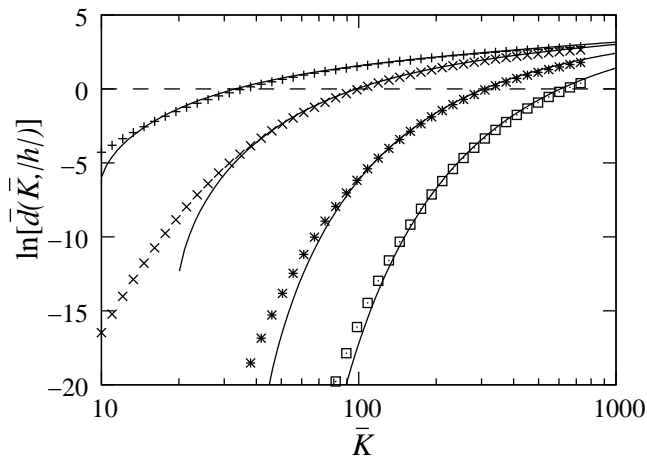


FIG. 5: Logarithm of the average damage,  $\ln[\bar{d}(\bar{K})]$ , as calculated from the annealed approximation, for different values of  $|h|$  ( $|h| = 10$  (+),  $|h| = 20$  (X),  $|h| = 40$  (\*) and  $|h| = 60$  (□)). The corresponding solid curves are obtained from Eq. (14). For not too small  $\bar{K}$ , one finds that Eq. (14) approximates the true damage function very well.

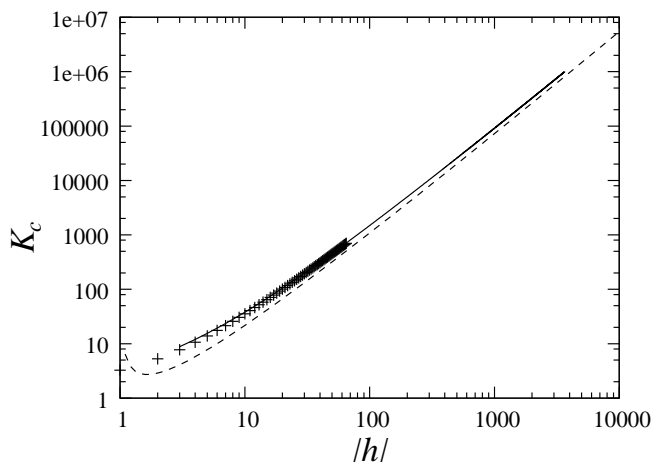


FIG. 6: Scaling behavior of the critical connectivity  $K_c(|h|)$  as a function of the (homogeneous) node threshold  $|h|$ , log-log-plot. Data points + are solutions obtained from the annealed approximation of Eq. (13), the solid curve is obtained from setting Eq. (14) to zero. The dashed line shows the asymptotic scaling behavior stated in Eq. (9).

impossible for  $|h| > 80$  due to exponentially diverging computing time caused by evaluation of the sum in Eq. (13) for large  $\bar{K}$  [36]. For estimation of the scaling behavior of  $K_c(|h|)$  for larger  $|h|$ , we are interested in a good approximation that does not require summation over the whole network topology, and hence neglect the variation in  $k$ , considering damage propagation in the *mean field limit*  $k = \text{const.} \approx \bar{K}$  (for details, see Appendix B). Using the Stirling approximation:  $n! \approx n^n e^{-n} \sqrt{2\pi n}$ , this leads to the following approximation for the logarithm of

the damage:

$$\ln[\bar{d}(\bar{K}, |h|)] \approx \frac{1}{2} \left\{ \ln \bar{K} - \bar{K} \cdot \ln \left[ 1 - \left( \frac{|h|}{\bar{K}} \right)^2 \right] \right. \\ \left. - |h| \ln \left[ \frac{\bar{K} + |h|}{\bar{K} - |h|} \right] \right\} + C \quad (14)$$

with  $C = \ln(\sqrt{2/\pi})$ ; solving this equation for

$$\ln[\bar{d}(K_c(|h|), |h|)] = 0 \quad (15)$$

then yields the critical connectivity  $K_c(|h|)$ . Figure 5 shows that this approximation is very accurate even for considerably small, finite  $|h|$ . In particular, one can show that for  $|h| \geq 10$  the relative error  $\epsilon$  between the approximation of Eq. (15) and the result obtained from the annealed approximation vanishes  $\sim |h|^{-1}$  (Fig. 7).

Still, Eq. (15) has to be solved numerically to calculate  $K_c(|h|)$ , and hence does not yield information about the scaling behavior in the limit  $|h| \rightarrow \infty$ . A first insight into the expected scaling can be obtained from an analysis of the scaling behavior of the maximum of  $p_s(k, |h|)$  with respect to  $|h|$ ; if we restrict our analysis to even  $k - |h|$ ,  $k_{max}$  is given by the condition

$$\Delta p_s = p_s(k, |h|) - p_s(k-2, |h|) \approx 0 \quad (16)$$

or, more accurately, we have to find the minimum of the absolute value  $|\Delta p_s / \Delta k|$  of the 'discrete derivative' of  $p_s(k, |h|)$  for even  $k - |h|$ , with  $\Delta k = \text{const.} = 2$ . Inserting Eq. (8) then yields

$$\Delta p_s = 2^{-k+3} \frac{(k-3)!}{[(k+|h|-3)/2]! [(k-|h|-3)/2]!} \cdot \left\{ \frac{(k-1)(k-2)}{(k+|h|+1)(k-|h|-1)} - 1 \right\}. \quad (17)$$

Obviously, the pre-factor on the right hand-side is always positive; consequently, in order to determine the maximum of  $p_s(k, |h|)$ , we have to solve the equation

$$\frac{(k-1)(k-2)}{(k+|h|+1)(k-|h|-1)} - 1 = 0. \quad (18)$$

Using simple algebra, one can show that

$$k_{max} = |h|^2 + 1 \quad (19)$$

solves this equation, i.e. the maximum of  $p_s(k, |h|)$  scales quadratically with  $|h|$ . Since  $p_s(k, |h|)$  for  $|h| \gg 0$  vanishes both for small and large  $k$ , it is plausible that the scaling behavior of  $K_c$  is dominated by the leading behavior of the maximum of the distribution, i.e. should scale  $\sim f(|h|)|h|^2$ , where contributions from the tails of the distribution are considered in  $f(|h|)$ .

A more detailed analysis carried out in appendix C takes into account that, for large  $\bar{K}$  and  $|h|$ , according to the central limit theorem the Binomial distribution

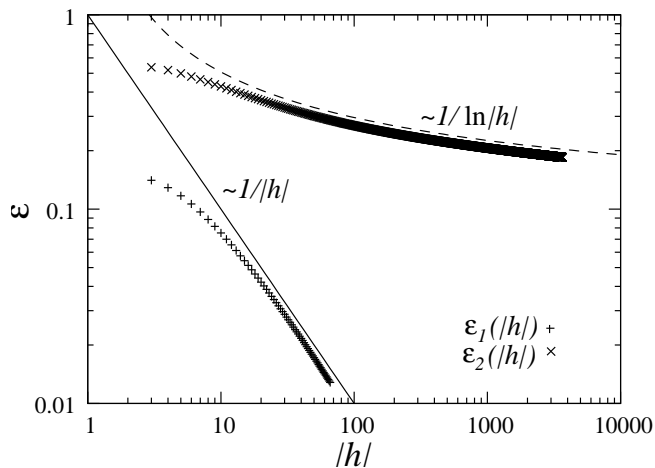


FIG. 7: Crosses (X): Relative error  $\varepsilon_1$  between the approximation of Eq. (14) and the result obtained from the annealed approximation, as a function of  $|h|$ . For  $|h| \geq 15$ ,  $\varepsilon_1$  vanishes  $\propto |h|^{-1}$ ; straight line with slope  $-1$  shown for comparison. Data points (+): Relative error  $\varepsilon_2$  between the approximation of Eq. (14) and the asymptotic scaling of Eq. (21);  $\varepsilon_2$  goes to zero logarithmically (compare to dashed curve).

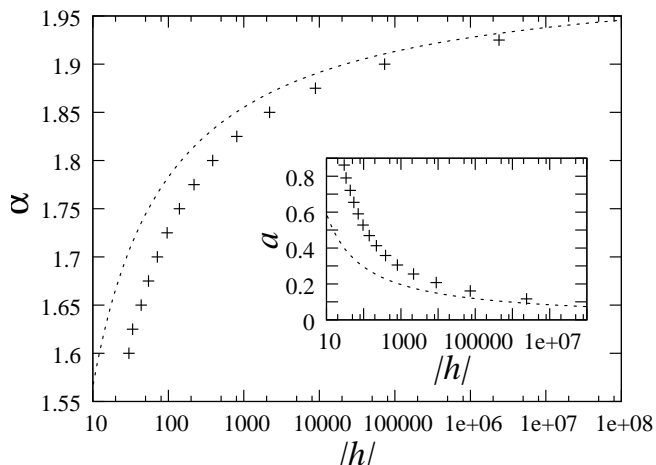


FIG. 8: Optimal exponents  $\alpha$  of power-laws  $K_c \approx a|h|^\alpha$  that approximate the scaling function  $K_c(|h|)$ , as shown in Fig. 6, as a function of  $|h|$ . The dashed curves are the corresponding asymptotic estimates of Eq. (23) and Eq. (24).

that characterizes the damage propagation function Eq. (8) can be replaced by a Gaussian, consequently, the expected damage is approximated very well by

$$\bar{d}(\bar{K}, |h|) = \bar{K} \cdot \sqrt{\frac{1}{2\pi\bar{K}}} \exp\left[-\frac{h^2}{2\bar{K}}\right]. \quad (20)$$

Taking logarithms and inserting into Eq. (15) then yields the asymptotic scaling

$$\lim_{|h| \rightarrow \infty} K_c(|h|) = \frac{h^2}{2 \ln |h|} \quad (21)$$

of the critical connectivity  $K_c$ . Figure 6 demonstrates the convergence of the critical line (straight-lined curve and data points) against this asymptote (dashed curve).

For finite  $|h|$ , we notice that there are substantial contributions from additional terms that vanish only logarithmically, and hence an approximation based on Eq. (21) would substantially underestimate  $K_c$ . This can be appreciated clearly from Fig. 7, which demonstrates the slow (logarithmic) convergence of the error  $\varepsilon_2(|h|)$  made by application of Eq. (21) for finite  $|h|$ .

From Fig. 6, it is also evident that, for finite  $|h|$ , Eq. (21) overestimates the slope  $dK_c/d|h|$ . One can show that, for finite  $|h|$ ,  $K_c(|h|)$  is better approximated locally by power-laws of the form

$$K_c(|h|) \approx a(|h|) \cdot |h|^{\alpha(|h|)} \quad (22)$$

with  $3/2 < \alpha < 2$ . We confirmed this intuition by numerically inserting candidate solutions with fixed  $\alpha$  into Eq. (14), and solving for the values of  $|h|$  and  $a$  where the deviation from the true curve  $K_c(|h|)$  becomes minimal; inverting this relation, we obtain the optimal power law exponents  $\alpha(|h|)$  as a function of  $|h|$  (Fig. 8, for details, see appendix E). Again, we can apply the Gaussian approximation for the damage propagation function to derive upper (lower) bounds for the finite size scaling of  $\alpha(|h|)$  and  $a(|h|)$ , which yield (cf. appendix E)

$$\alpha(|h|) \approx 2 - \frac{1}{\ln |h|}, \quad (23)$$

and

$$a(|h|) \approx \frac{e}{2 \ln |h|}. \quad (24)$$

Figure 8 shows that the true optimal values are systematically below ( $\alpha$ ) or above ( $a$ ) these curves, demonstrating the non-trivial scaling behavior of the critical line for finite  $|h|$ , which is significantly different from the simple asymptotic behavior in the thermodynamic limit (Eq. (21)).

Let us now investigate the scaling behavior of  $K_c$  for networks with inhomogeneous thresholds. Figure 9 shows that, for finite  $|h|$ , the critical line  $K_c(|h|)$  for RTN with inhomogeneous thresholds is always *below* the corresponding values for homogeneous  $|h|$ ; the absolute *difference*  $\Delta K_c(|h|) := |K_c^h(|h|) - K_c^i(|h|)|$  between both curves, however, increases only linearly in with  $|h|$  (inset of Fig. 9), where  $K_c^h(|h|)$  is the critical connectivity for homogeneous  $|h|$ , and  $K_c^i(|h|)$  the corresponding value for inhomogeneously distributed  $|h|$  with mean  $|\bar{h}| = |h|$ .

Intuitively, this is straight-forward to understand: since we assumed that  $k$  and  $|h|$  are *statistically independent*,  $\Delta K_c(|h|)$  is determined solely by the *variance*  $\sigma_h^2$  of the threshold distribution around the mean threshold  $|\bar{h}| = |h|$  - the smaller this variance is, the more peaked this distribution is around  $|\bar{h}| = |h|$ , and the less it hence differs from the homogeneous distribution. Since we assumed that (in the inhomogeneous case) thresholds are

Poisson distributed around  $|\bar{h}|$ , we directly conclude

$$\Delta K_c(|h|) \sim \sigma_h^2 = |\bar{h}|. \quad (25)$$

For arbitrary threshold distributions that are statistically independent from the networks' degree distribution with variance  $\sigma_k^2$ , we make the ansatz

$$\sigma_{tot}^2 = \sigma_k^2 + \sigma_h^2 \quad (26)$$

for the total variance  $\sigma_{tot}^2$ . Using the same Gaussian approximation as above for the homogeneous case, one can show that

$$K_c(|\bar{h}|) \approx \frac{\bar{h}^2}{2 \ln |\bar{h}|} - \sigma_h^2 \quad (27)$$

for networks with inhomogeneous thresholds distributed around an average absolute threshold  $|\bar{h}|$  (for details, cf. appendix C). This implies that, in the limit  $|\bar{h}| \rightarrow \infty$ , all networks with Poissonian distributed connectivity and threshold distributions with a variance which obeys the scaling relation:  $\sigma_h^2 \sim |\bar{h}|^\beta$  with  $0 \leq \beta < 2$ , follow the universal asymptotic scaling relation

$$K_c(|\bar{h}|) = \frac{\bar{h}^2}{2 \ln |\bar{h}|}, \quad (28)$$

as it is shown in appendix C. This means that in all these cases, the asymptotic scaling for  $|\bar{h}| \rightarrow \infty$  is dominated by the scaling behavior of the maximum of the damage propagation function  $p_s(k, |h|)$ , with an exponent  $\alpha = 2$ .

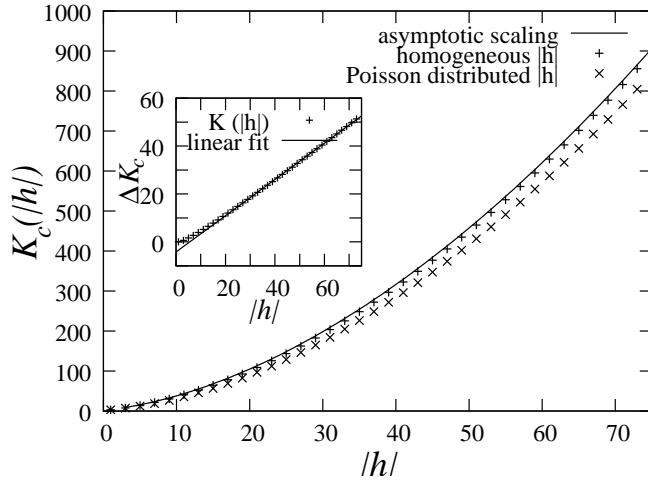


FIG. 9:  $K_c(|h|)$  for homogeneous thresholds (+) and Poisson distributed thresholds with the same average  $|\bar{h}|$  (X), annealed approximation. The solid line is the asymptotic scaling obtained from Eq. (15). For inhomogeneous  $|h|$ , the critical line is systematically below  $K_c$  of networks with homogeneous  $|h|$ . *Inset*: The difference  $|\Delta K_c(|h|)|$  between both curves grows only linearly in  $|h|$ , confirming that the asymptotic scaling in the limit  $|h| \rightarrow \infty$ , is the same in both cases.

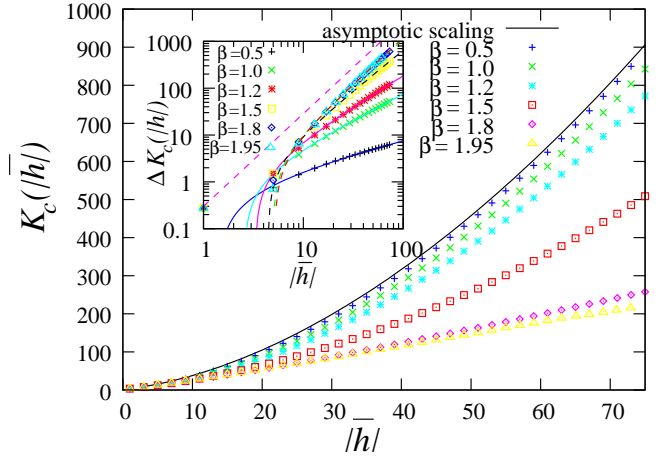


FIG. 10:  $K_c(\beta, |\bar{h}|)$  for networks with threshold distributions following discretized Gaussian distributions with different variances  $Var(|h|) = |\bar{h}|^\beta$  (for details, see text). One clearly appreciates that the larger the variance of the threshold distribution, the more the curves  $K_c(\beta, |\bar{h}|)$  are below the critical line of networks with homogeneous thresholds (blue solid line); in the limiting case  $\beta = 1.95 \approx \alpha$  (yellow triangles),  $K_c$  scales almost linearly with  $|\bar{h}|$ . *Inset*: differences  $|\Delta K_c(\beta, |\bar{h}|)|$  to the critical line of RTN with homogeneous thresholds scale  $\sim |\bar{h}|^{\beta_e}$  with  $\beta < \beta_e < \alpha$  (power law fits and dashed line with slope  $\alpha$  shown for comparison); this implies asymptotic convergence to the universal scaling function Eq. (28) in the limit  $|h| \rightarrow \infty$  for all cases shown here.

$\beta$	$\beta_e$
0.5	$0.533 \pm 0.009$
1.0	$1.099 \pm 0.004$
1.2	$1.327 \pm 0.004$
1.5	$1.732 \pm 0.004$
1.8	$1.942 \pm 0.003$
1.95	$1.975 \pm 0.004$

TABLE I: Scaling exponents  $\beta_e$ , as obtained from fits of  $\Delta K_c \sim |\bar{h}|^{\beta_e}$ , as a function of  $\beta$ .

Let us now confirm this finding for a different class of threshold distributions. Since in a Poissonian the variance is not a free parameter, we now instead choose a discretized Gaussian distribution, i.e.

$$P(|h|) = \frac{Z}{\sigma_h \sqrt{2\pi}} e^{-\frac{1}{2}(|h| - |\bar{h}|)^2 / \sigma_h^2} \quad (29)$$

with

$$Z = \left\{ \sum_{|h|=0}^{|\bar{h}|_m} \frac{1}{\sigma_h \sqrt{2\pi}} e^{-\frac{1}{2}(|h| - |\bar{h}|)^2 / \sigma_h^2} \right\}^{-1} \quad (30)$$

and variance

$$\sigma_h^2 = |\bar{h}|^\beta, \quad \beta \in [0, \alpha]. \quad (31)$$

The factor  $Z$  ensures that the probabilities are normalized in the interval  $[0, |h|_m]$ , where  $|h|_m$  denotes the cut-off of the threshold distribution. Figure 10 compares the scaling functions  $K_c(|\bar{h}|)$  for different values of  $\beta$  to the asymptotic case of homogeneous networks. Obviously, for finite  $|\bar{h}|$ , increased variance of the threshold distribution substantially lowers the critical connectivity; in the limiting case  $\beta \approx \alpha$ ,  $K_c$  grows only linearly with  $|\bar{h}|$ . For  $\beta < \alpha$ , we find that the deviation from the scaling behavior of RTN with homogeneous thresholds scales as

$$\Delta K_c \propto |\bar{h}|^{\beta_e}. \quad (32)$$

Table 1 compares  $\beta$  and  $\beta_e$  (as obtained from fits of  $\Delta K_c$ ; in all cases, we have  $\beta_e > \beta$ , which is a discretization effect, but still  $\beta_e < \alpha$ . Hence, it follows that

$$\begin{aligned} \lim_{|h| \rightarrow \infty} \frac{K_c(\beta, |\bar{h}| = |h|)}{K_c^h(|h|)} &= \lim_{|h| \rightarrow \infty} \frac{K_c^h(|h|) - \Delta K_c(\beta, |h|)}{K_c^h(|h|)} \\ &= 1 - \text{const.} \cdot \lim_{|h| \rightarrow \infty} |h|^{\beta_e - \alpha} \\ &= 1 \end{aligned} \quad (33)$$

for  $\beta_e < \alpha$ , i.e. in this case all scaling functions  $K_c(\beta, |\bar{h}|)$  for  $|h| \rightarrow \infty$  indeed asymptotically converge to the same universal scaling function, as given by Eq. (28).

Let us now have a closer look at the scaling behavior of the intersection points  $K_d(|h|)$ , as introduced in the last paragraph of subsection B. Let  $\bar{d}^h(\bar{K}, |h|)$  be the expected damage in networks with homogeneous threshold, and  $\bar{d}^i(\bar{K}, |h|)$  the expected damage in networks with inhomogeneous thresholds; then

$$\bar{d}^h(K_d(|h|), |h|) - \bar{d}^i(K_d(|h|), |\bar{h}|) = 0 \quad (34)$$

$$|\bar{h}| = |h| \quad (35)$$

are the defining equations for  $K_d(|h|)$ . Notice that for  $\bar{K} < K_d$ , the randomness introduced by inhomogeneous thresholds actually *increases* the probability for damage spreading, whereas for  $\bar{K} > K_d$ , it is *decreased*. Equation (34), under condition Eq. (35), can be solved numerically for not too large  $|h|$ . Further, one can derive the asymptotic scaling in the thermodynamic limit by application of the Gaussian approximation for the damage propagation function (for details, cf. appendix D), showing that

$$\lim_{|h| \rightarrow \infty} K_d(|h|) = h^2 - |h|. \quad (36)$$

Fig. 11 demonstrates that  $K_d(|h|)$  approaches this asymptotic scaling already for considerably small  $|h|$ , indicating that  $K_d(|h|)$  is characterized by the same universal scaling exponent  $\alpha = 2$  as  $K_c(|h|)$ . Notice, however, that the asymptotic scaling law for  $K_d$  obeys a purely algebraic relation, whereas  $K_c$  has a dependence  $\sim h^2 / \ln |h|$  (Eq. 21).

Let us briefly compare the scaling behavior of RTN with non-zero thresholds, as discussed above, to Random Boolean Networks (RBN). Obviously, increasing  $|h|$

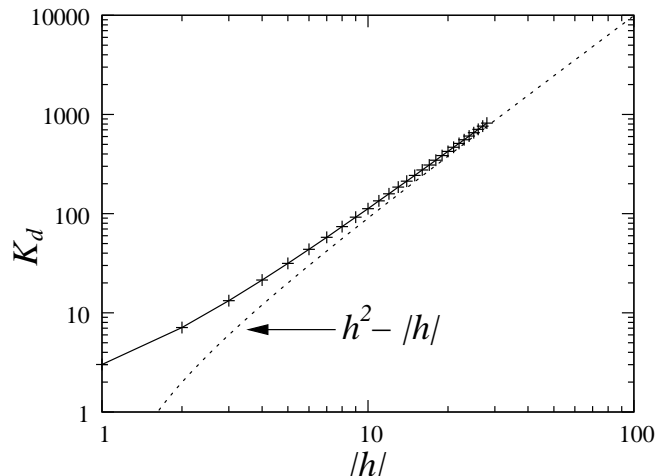


FIG. 11: Scaling behavior of  $K_d(|h|)$  as a function of  $|h|$ , double logarithmic plot. The dashed line highlights the asymptotic scaling (Eq. (36)).

biases the output states of network nodes (for the systems discussed in this paper, it increases the probability to have an output state  $\sigma_i = -1$ ). Biased RBN obey the scaling relationship [4]

$$K_c = \frac{1}{2p(1-p)}. \quad (37)$$

To compare this relationship to the asymptotic scaling for RTN in the limit of large  $|h|$ , we have to consider the limit  $p \rightarrow 1$ . One can show that, in this limit, the scaling function Eq. (37) logarithmically approaches the asymptotic scaling

$$K_c \approx -\frac{p^2}{2 \ln p}. \quad (38)$$

This shows that  $|h|$  plays the same role as the bias parameter  $p$  in RBN, and that both classes obey the same scaling in the limit  $p \rightarrow 1$  and  $|h| \rightarrow \infty$ , respectively. However, there are also substantial differences between both classes of systems, that come into play when  $|h|$  is small (when  $p$  is close to 1/2). In particular, while RBN in this limit still obey the simple scaling relationship Eq. (37), the critical connectivity  $K_c$  of RTN is derived from the complex dependence of Eq. (14). This difference is due to the fact that, in RTN, local damage propagation strongly depends on the in-degree of nodes (cf. Eq. 6 and 8), while it is independent from the in-degree in RBN for  $k > 0$ . In the limit of sparsely connected networks (i.e. small  $|h|$  and  $K_c$ ), this leads to much stronger finite size effects in RTN than in RBN. Furthermore, in this limit also the absolute values of  $K_c$  in RTN are considerably below those of RBN [24, 25].

Finally, let us remark on the existence of the characteristic connectivity  $K_d$ . As shown above,  $K_d$  is defined for RTN with arbitrary  $|h|$ , in particular, it exists in the limit

$|h| \rightarrow \infty$ , with a well-defined asymptotic scaling. For biased RBN, the corresponding limit is given by  $p \rightarrow 1$  (or, equivalently,  $p \rightarrow 0$ ). Obviously, we can in principle assign variable (inhomogeneous) biases  $p_i$  to different RBN nodes such that the *average* bias is equal to  $p$ . However, because  $p$  is a probability and hence  $0 \leq p \leq 1$ , the variance  $\sigma_p^2$  has to vanish in the limit  $p \rightarrow 1$  ( $p \rightarrow 0$ ) to yield a proper average bias. Since  $K_d$  is defined by comparing networks with diverging variance of the order parameter  $|h|$  (or  $p$ , respectively) with the corresponding networks with vanishing variance and the same average  $|h|$  (or  $p$ , respectively), this implies that  $K_d$  is *not defined* for RBN in the limit of large bias  $p \rightarrow 1$ , which corresponds to  $|h| \rightarrow \infty$  in RTN. Hence,  $K_d$  constitutes a truly novel, not previously known concept, yielding a new characteristic connectivity which is well-defined only for RTN.

It is interesting to notice that the dependence of  $K_c$ , as well as of  $K_d$  on  $|h|$  is clearly super-linear even for considerably small  $|h|$ ; this has profound consequences for algorithms that evolve RTN towards (self-organized) criticality by local adaptations of both thresholds and the number of inputs a node receives from other nodes [32]. In particular, it can be shown that co-evolution of network dynamics and thresholds/in-degrees leads to strong correlations between  $|h|$  and  $k$ . To approach this type of problem analytically, we will now extend our analysis in this direction. first, In the next section, we will show that even weak correlations between  $k$  and  $|h|$  can lead to a transition from sub-critical to super-critical dynamics (and vice versa), while keeping the average connectivity  $\bar{K}$  and the average absolute threshold  $|h|$  constant.

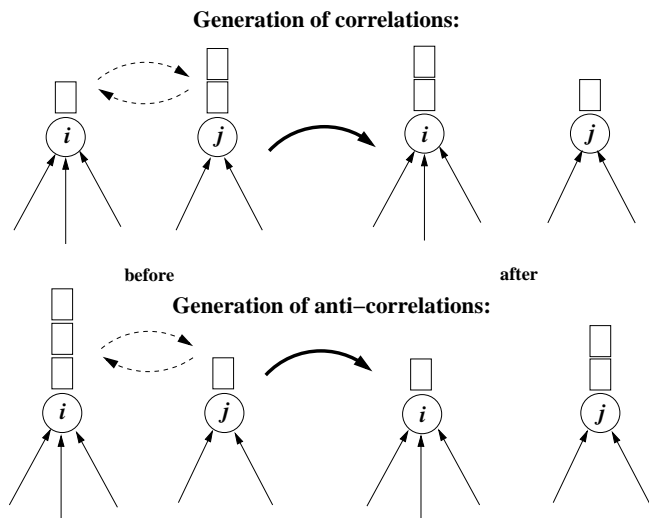


FIG. 12: Schematic illustration of the algorithm applied to generate local (anti-)correlations between in-degree  $k_{in}$  and (absolute) threshold  $|h|$ . Arrows symbolize inputs from other nodes, boxes symbolize node thresholds (one box corresponds to  $|h| = 1$ , two boxes to  $|h| = 2$ , and so on). For details of the algorithm, please refer to the text.

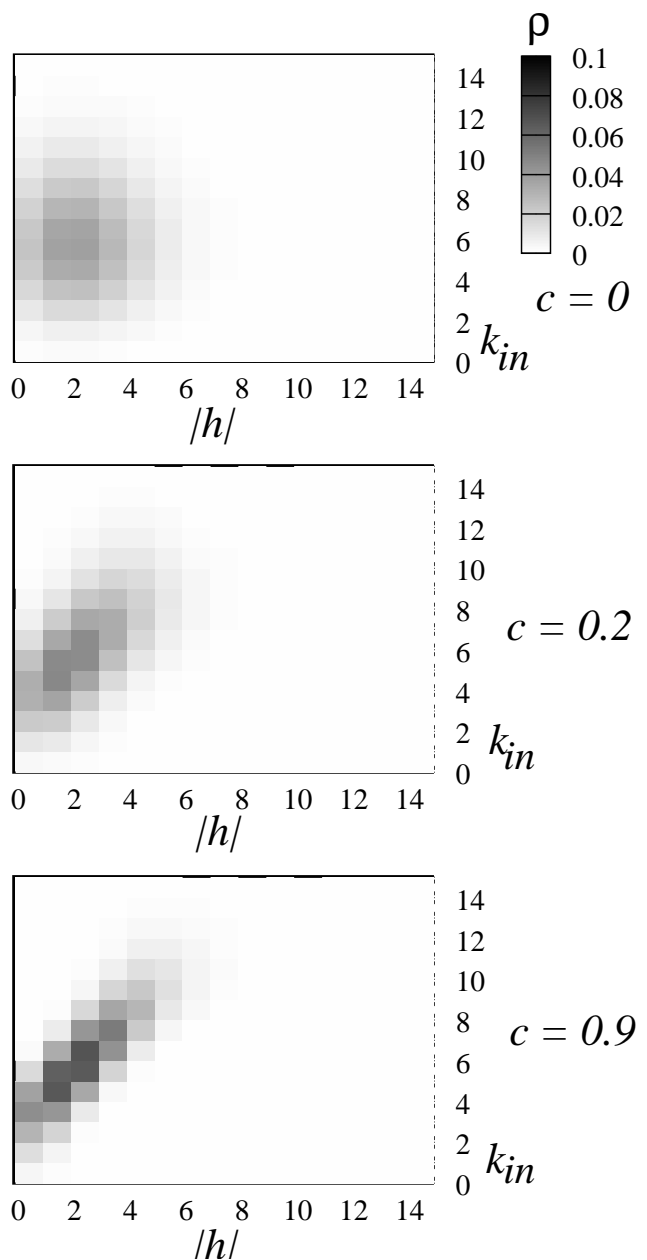


FIG. 13: Combined density  $\rho(k_{in}, |h|)$  for three different positive values of the correlation parameter  $c$ , from top to bottom:  $c = 0$ ,  $c = 0.2$  and  $c = 0.9$ . Dark gray indicates a high probability density. The diagonal structure of  $\rho(k_{in}, |h|)$  for  $c = 0.9$  (lower panel) indicates emergence of strong positive correlations between  $k_{in}$  and  $|h|$ .

#### D. Effect of correlations between $k$ and $h$

So far, we assumed that node degree and node thresholds are totally uncorrelated; while this matches well the "maximum disorder" assumption used in random ensemble based approaches as, e.g., the annealed approximation, this might be a quite unrealistic constraint for many

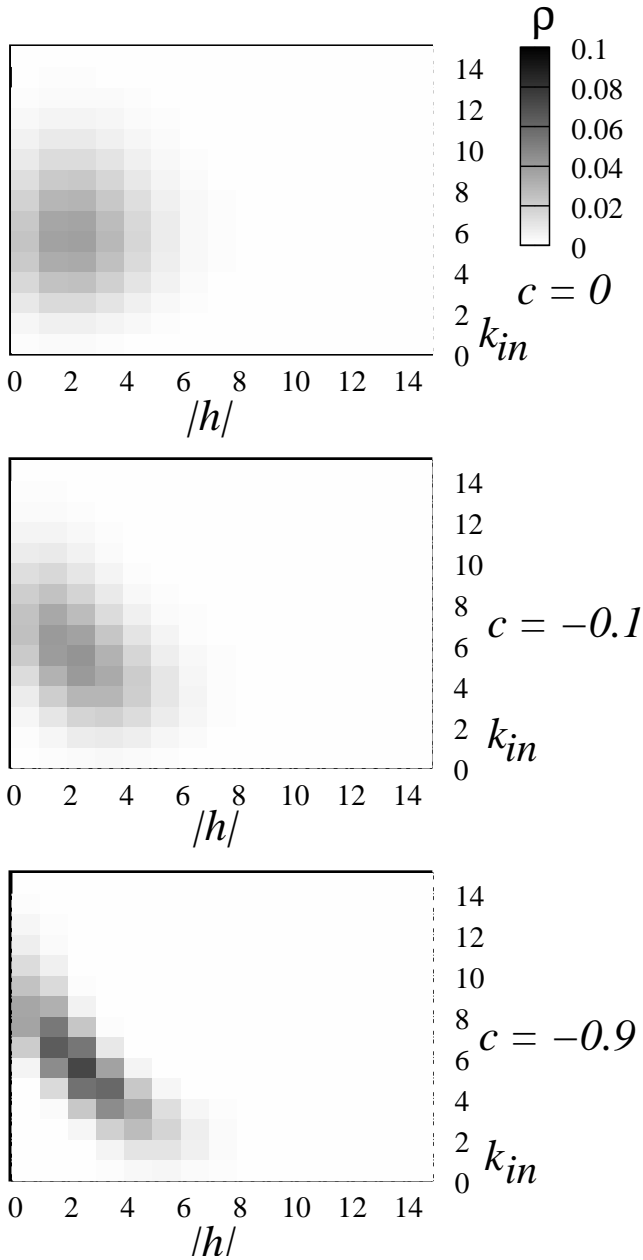


FIG. 14: Combined density  $\rho(k_{in}, |h|)$  for three different negative values of the correlation parameter  $c$ , from top to bottom:  $c = 0$ ,  $c = -0.1$  and  $c = -0.9$ . Dark gray indicates a high probability density. The inverted diagonal structure of  $\rho(k_{in}, |h|)$  for  $c = -0.9$  (lower panel) indicates emergence of strong anti-correlations between  $k_{in}$  and  $|h|$ .

real world networks. Indeed, one can show that even in a simple evolutionary algorithm that couples both the adaptation of node thresholds  $h_i$  and in-degree  $k_i$  to a local dynamical order parameter, strong correlations between both quantities emerge spontaneously [32]. Hence, it is an interesting question to ask whether correlations (or anti-correlations) between  $h$  and  $k$  may induce a transition from sub-critical to super-critical networks (or vice

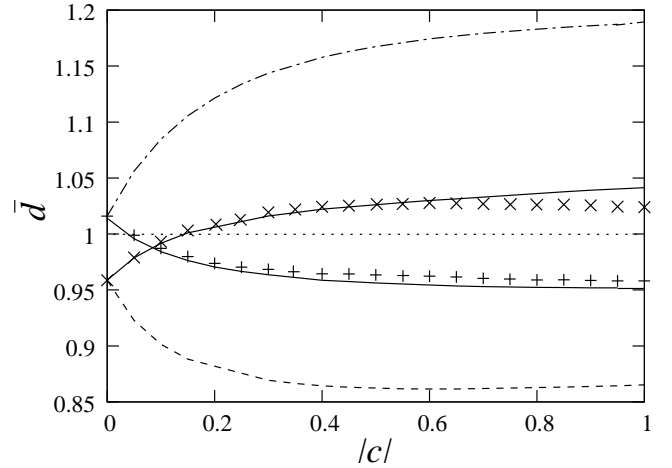


FIG. 15: Average damage  $\bar{d}(c)$  as a function of  $|c|$ , for correlated  $k_{in}$  and  $|h|$  (+) and anti-correlated  $k_{in}$  and  $|h|$  (X), with  $\bar{K} = 6.15$  for  $c \geq 0$  networks and  $\bar{K} = 5.8$  for  $c \leq 0$  networks and  $|\bar{h}| = 2.5$  in both cases. Numerical data were obtained from ensemble averages over  $Z = 5 \cdot 10^5$  randomly generated RTN with  $N = 1024$  nodes for each data point. Solid curves are the corresponding results of the *corrected* annealed approximation, while the dashed-dotted curve shows the uncorrected result for correlated  $in k$  and  $|h|$ , and the dashed curve the uncorrected result for anti-correlated  $k_{in}$  and  $|h|$ , respectively.

versa), while we keep  $\bar{K}$  and  $|\bar{h}|$ , and network topologies constant.

Let us first formulate an algorithm that generates correlations (anti-correlations) between  $k$  and  $|h|$ . For this purpose, a parameter  $c \in [0, 1]$  is introduced which parameterizes the probability that  $k$  and  $|h|$  are locally correlated (anti-correlated). The topology-generating algorithm then reads as follows (compare also Fig. 12):

- 1) Generate a random, directed network with Poisson distributed  $k$  and Poisson distributed  $|h|$  with average connectivity  $\bar{K}$  and  $|\bar{h}|$  for all sites.
- 2) Select a pair of sites  $i \leq N$  and  $j \leq N$  at random.  $c > 0$ : exchange the sites' thresholds if  $k_{in}(i) \geq k_{in}(j)$  and  $|h|(i) \leq |h|(j)$ , or vice versa.  $c < 0$ : exchange the sites' thresholds if  $k_{in}(i) \leq k_{in}(j)$  and  $|h|(i) \leq |h|(j)$ , or vice versa.
- 3) Go back to 2) and repeat the algorithm for  $c \times P_{max}$  steps, where  $P_{max}$  is a pre-defined maximum number of correlated pairs.

Obviously, increasing the parameter  $c \in [0, 1]$  increases correlations (anti-correlations) between  $k_{in}$  and  $h$ . If we repeat this algorithm  $Z$  times for fixed  $c$ , we can generate a random ensemble of  $Z$  correlated/anti-correlated networks, and investigate damage spreading on these networks. The ensemble-averaged probability  $\rho(k_{in}, |h|)$  to have a site with  $k_{in}$  inputs and threshold  $|h_i| = |h|$  then

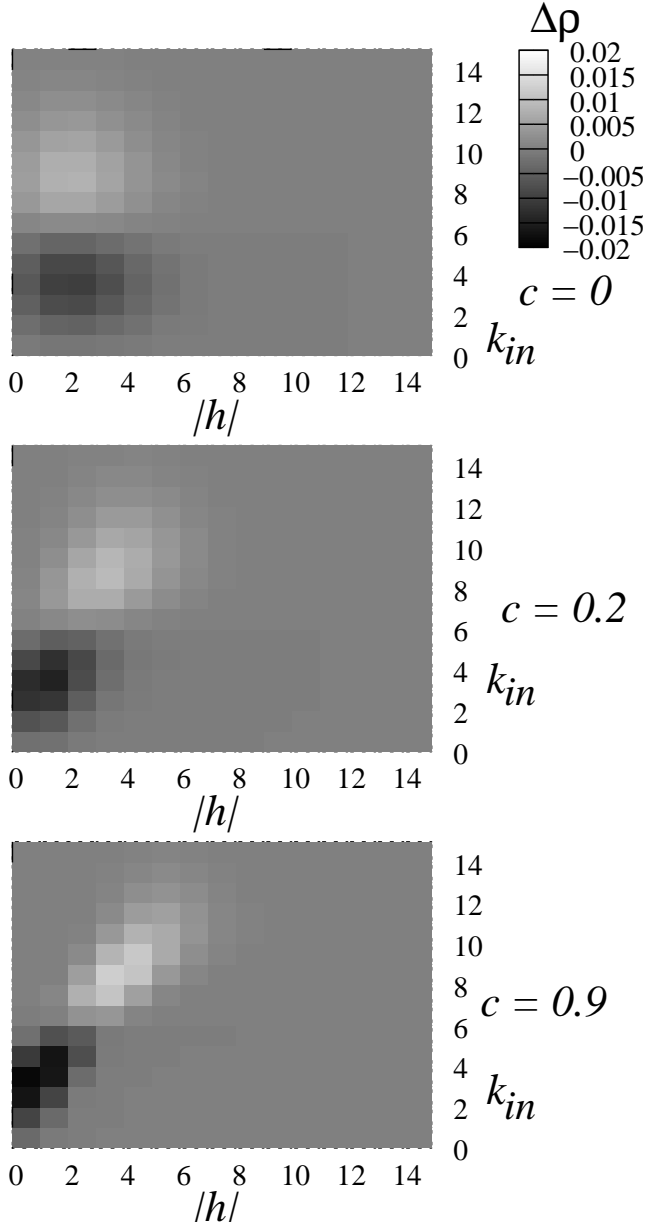


FIG. 16: Difference  $\Delta\rho(k, |h|)$  between real and effective combined densities (see text), for three different values of positive  $c$ . Dark gray indicates a negative deviation, light gray positive deviation, a medium intensity refers to zero deviation.

is defined as

$$\rho(k_{in}, |h|) = \frac{\sum_{j=1}^Z n_j(k_{in}, |h|)}{Z \cdot N}, \quad (39)$$

where  $n_j(k_{in}, |h|)$  is the number of sites with  $k_{in}$  inputs and threshold  $|h_i| = |h|$  in the  $j$ th random network. Figure 13 demonstrates the correlating effect of the algorithm on the *average* probabilities  $\rho(k_{in}, |h|)$  for ensembles of  $10^5$  randomly generated networks, for the case  $c \geq 0$ , with  $P_{max} = 10^4$ . For  $c = 0$ , clearly no cor-

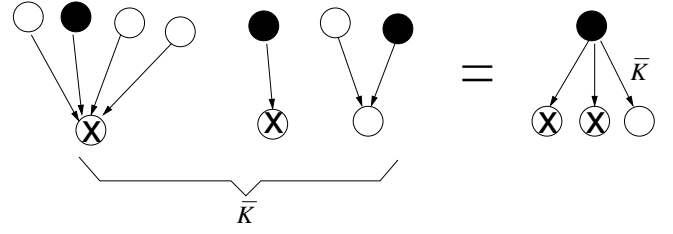


FIG. 17: Schematic illustration of the *naive* mean-field assumption implicit to the annealed approximation: Choosing a random ensemble of  $\bar{K}$  nodes and inverting one input of each of them (left panel, black circles refer to inverted states) on average yields the same damage as perturbing a randomly chosen site with  $\bar{K}$  outputs and investigating the resulting damage at the output nodes (right panel); in both panels, X means "damaged states". This assumption is violated for correlated networks, even if the generating algorithm *explicitly* correlates only in-degree and thresholds.

relations are present, and the combined density simply represents the independent superposition of the two underlying Poisson distributions. With increasing  $c$ , correlations gradually emerge, and for  $c = 0.9$  the resulting distribution clearly exhibits a diagonal structure. Figure 14 demonstrates the corresponding effect for  $c \leq 0$ , i.e. anti-correlated topologies.

Let us now investigate how these correlations affect damage propagation. To apply the annealed approximation, we now have to calculate the average probability for damage propagation (in a finite network of size  $N$ ) according to

$$\langle p_s \rangle(\bar{K}, |\bar{h}|, c) = \sum_{|h|=0}^{|\bar{h}|_m} \sum_{k=|h|}^N \rho(k_{in}, |h|) p_s(k+1, |h|), \quad (40)$$

with the normalization conditions

$$\sum_{|h|=0}^{|\bar{h}|_m} \sum_{k=|h|}^N \rho(k_{in}, |h|) = 1 \quad (41)$$

and

$$\sum_{|h|=0}^{|\bar{h}|_m} \sum_{k=|h|}^N |h| \rho(k_{in}, |h|) = |\bar{h}|, \quad (42)$$

where  $|\bar{h}|_m$  is the maximal absolute threshold observed (cutoff); correlations enter via the probabilities  $\rho(k_{in}, |h|)$  to observe a node with in-degree  $k_{in}$  and absolute threshold  $|h|$ .

Figure 15 compares the numerically observed damage  $\bar{d}$  (for ensembles of randomly generated networks) one time step after a one-bit perturbation to the expected damage  $\langle p_s \rangle(\bar{K}, |\bar{h}|, c) \cdot \bar{K}$ , as predicted by the annealed approximation (dashed curves). In both cases, for correlations and anti-correlations, the so-obtained theoretical

curves are obviously wrong both with regard to quantitative matching of the numerical data, as with regard to the predicted trend: while in the numerical experiment a decrease of  $\bar{d}$  with increasing  $c > 0$  is observed, i.e. a transition from super-critical (chaotic) to sub-critical (ordered) dynamics, the annealed curve predicts a strong increase. Corresponding observations (with opposite signs) are made for the case of anti-correlations. We conclude that there must be an additional effect present which is not captured in our *naive mean-field model*. To identify the origin of this deviation, one has to compare the distribution  $\tilde{\rho}(k_{in}, |h|)$  which is observed for the *outputs of perturbed sites* with the original distribution  $\rho(k_{in}, |h|)$ , which is averaged over the whole topology. Figure 16 shows the deviation  $\Delta\rho(k_{in}, |h|) := \tilde{\rho}(k_{in}, |h|) - \rho(k_{in}, |h|)$  between both distributions. While for small  $k_{in}$  and  $|h|$  negative deviations are found, for larger  $k_{in}$  and  $|h|$  deviations have a positive sign. One can easily understand the source of this *effective bias*, when one thinks of the correlation-generating mechanism (Fig. 12): if we pick, by chance, within a correlated network a site  $i$  with small  $k_{in}$ , it will probably also have a small  $|h|$ , and its outputs will probably have *larger*  $k_{in}$  and  $|h|$  than site  $i$ . Since both  $k_{in}$  and  $|h|$  are bounded from below, this leads to a systematic bias to observe larger  $k_{in}$  and  $|h|$ , at the expense of smaller, for the outputs of perturbed nodes. The opposite effect obviously holds for sites with large  $k_{in}$  and  $|h|$ . While for  $c = 0$  this effect is very small, it becomes dominant for  $c \rightarrow 1$  due to the strong asymmetry of the diagonal distribution. If we correct the annealed approximation to include this bias, by replacing  $\rho(k_{in}, |h|)$  with  $\tilde{\rho}(k_{in}, |h|)$  in Eq. (40), we find that the resulting *corrected* annealed curves much better match the numerically observed damage (still, there are slight discrepancies for large  $c$ , which are due to finite ensemble sizes).

The result of this study demonstrates that the annealed approximation has to be used with extreme care, when topological correlations are present. Although the applied algorithm *explicitly* correlates only in-degree and thresholds, consideration of these correlations only by using a combined density  $\rho(k_{in}, |h|)$  for averages over topology and dynamics leads to wrong predictions. In addition, one has to consider systematic bias effects between perturbed sites and their outputs, which arise as a side effect of the correlating algorithm. This shows that the naive mean-field assumption inherent to the annealed approximation, as demonstrated in Fig. 17, is violated even in the simplest case of correlations between in-degree and thresholds. Instead, complete information about topology, including the output side, has to enter statistics, and the order of averages becomes important.

#### IV. DISCUSSION

An increasing number of studies is concerned with the propagation dynamics of perturbations and/or informa-

tion in complex dynamical networks. Discrete dynamical networks, in particular Random Boolean Networks (RBN) and Random Threshold Networks (RTN), constitute an ideal testbed for this type of question, since they are easily accessible for both computational methods and the tool boxes of statistics and combinatorics. Often, it is found that damage/information propagation strongly depends on the type of inhomogeneities present in network wiring. Several studies focus, for example, on the effect of scale-free degree distributions [25, 26]. Typically, these studies employ mean-field methods and hence represent, in a sense, strongly idealized models, since they derive results that strictly hold in the thermodynamic limit only.

Consequently, a second line of research concentrates on modification of damage propagation due to finite-size effects, which play a decisive role in many real-world networks. Recently, it was shown that weakly perturbed, finite size RBN and RTN show pronounced deviations from the annealed approximation [11]. Fronczak and Fronczak showed that these deviations can be explained by inhomogeneities and emergent correlations found at the percolation transition [33], however, their study is currently limited to undirected networks. In this context, the system discussed in our paper constitutes a complementary approach: it allows to introduce *dynamical inhomogeneity* of network units, without otherwise altering network topology. While this type of dynamical diversity certainly plays an important role in many real-world networks, it is neglected by most researchers. Let us now briefly summarize the main results of our study.

We studied damage propagation in Random Threshold Networks (RTN) with homogeneous and inhomogeneous negative thresholds, both analytically (using an annealed approximation) and in numerical simulations. We derived the probability  $p_s(k, |h|)$  of damage propagation for arbitrary in-degree  $k$  and (absolute) threshold  $|h|$  (Eqs. (5)-(8)), and, from this, the corresponding *annealed* probabilities  $\langle p_s \rangle$  (Eq. (10) and Eq. (12)) and the expected damage  $\bar{d}$  (Eq. (11)), for both the cases of homogeneous and inhomogeneously distributed thresholds. On these grounds, we investigated the scaling behavior of the critical connectivity  $K_c$  as a function of  $|h|$ . Using a mean field approximation, a simplified scaling equation for the logarithm of the average damage was derived (Eq. (14)), and applied to derive the critical line  $K_c(|h|)$  (Fig. 6). It was shown that this function exhibits a super-linear increase with  $|h|$ , which asymptotically approaches a unique scaling law  $K_c(|h|) \sim h^2 / (2 \ln |h|)$  for large  $|h|$  (Eq. (18) and Fig. 7). However, convergence against this asymptotic scaling is very slow (logarithmic in  $|h|$ ), which indicates that finite size effects are very dominant, and cannot be neglected for realistically sized networks. We presented evidence that this asymptotic scaling is universal for RTN with Poissonian distributed connectivity and threshold distributions with a variance that grows slower than  $h^2$ , for both the cases of Poisson distributed thresholds (Fig. 8) and thresholds distributed according

to a discretized Gaussian (Fig. 9). Interestingly, inhomogeneity in thresholds, meaning that each site has an individual threshold  $|h_i|$  drawn, e.g., from a Poisson distribution with mean  $|h|$ , increases damage for small average connectivity  $\bar{K}$ , when compared to homogeneous networks with the same average threshold  $|h| = \bar{h}$ , whereas for larger  $\bar{K}$  with  $\bar{K} > K_d$ , damage is reduced. This establishes a new characteristic connectivity  $K_d(|h|)$  with  $K_d > K_c$ , that describes the ambivalent effect of threshold inhomogeneity on RTN dynamics. We showed that  $K_d(|h|)$  asymptotically converges against a unique scaling law  $K_d \sim h^2$  in the limit  $|h| \rightarrow \infty$ . The scaling of  $K_d$  was compared to the corresponding case of random Boolean networks (RBN) with inhomogeneously distributed bias, parameterized in terms of a bias parameter  $1/2 \leq p \leq 1$ . It was shown that  $K_d$  is not defined for RBN in the limit  $p \rightarrow 1$ , which corresponds to  $|h| \rightarrow \infty$  in RTN. Hence,  $K_d$  constitutes a truly novel, not previously known concept, yielding a new characteristic connectivity which is well-defined only for RTN.

Last, we introduced local correlations between in-degree  $k_{in}$  of network nodes and their (absolute) threshold  $|h|$ , while keeping all other network parameters constant. We found that even small positive correlations can induce a transition from supercritical (chaotic) to subcritical (ordered) dynamics, while anti-correlations have the opposite effect. It was shown that the naive mean-field assumption typical for the annealed approximation leads to false predictions in this case. Even in the simplest case, where only in-degree and (absolute) threshold are correlated, complete information about topology, including the output side, has to enter statistics, and the

order of averages becomes important.

To summarize, dynamics of damage (or information) propagation in RTN with inhomogeneous thresholds and Poisson distributed connectivity shows both similarities and differences, when compared to networks with homogeneous thresholds: similarities manifest themselves in common universal scaling functions for both  $K_c$  and  $K_d$ , whereas differences show up in the opposite effects of threshold inhomogeneity for small and large  $\bar{K}$ . Differences become even more prominent in networks that are characterized by correlations between in-degree and thresholds. In this case, the annealed approximation has to be used with extreme care. Many dynamical systems in nature, that can be described as complex networks, exhibit considerable variation of activation thresholds among the elements they consist of, however, these variations are often neglected (e.g., in Boolean network based models of gene regulation networks). Our results indicate that, while general characteristics as, for example, the scaling behavior of critical points, may be conserved in approximations of this type, inhomogeneous thresholds can strongly impact the details of network dynamics, and hence should be taken into account in models that aim to give a realistic description of the dynamics of, e.g., gene regulation networks.

## V. ACKNOWLEDGMENTS

The author thanks A. Hübler for interesting discussions and careful reading of the manuscript, and acknowledges significant contributions of an anonymous referee with regard to the discussion of scaling behavior.

- 
- [1] S.A. Kauffman, *J. Theor. Biol.* **22**, 437 (1969)
  - [2] S.A. Kauffman, *The Origins of Order: Self-Organization and Selection in Evolution*, Oxford University Press, 1993.
  - [3] B. Derrida and Y. Pomeau, *Europhys. Lett.* **1** (1986) 45-49
  - [4] B. Derrida, in *Fundamental Problems in Statistical Mechanics VII*, edited by H. van Beijeren (North-Holland, Amsterdam, 1990)
  - [5] R. V. Solé and B. Luque, *Phys. Lett. A* **196** (1995), 331-334
  - [6] B. Luque and R. V. Solé, *Phys. Rev. E* **55** (1997), 257-260
  - [7] B. Samuelsson and C. Troein, *Phys. Rev. Lett.* **90**, 098701 (2003)
  - [8] R. Albert and A. L. Barabási, *Phys. Rev. Lett.* **84**, 5660 (2000)
  - [9] V. Kaufman, T. Mihaljev and B. Drossel, *Phys. Rev. E* **72**, 046124 (2005)
  - [10] T. Mihaljev and B. Drossel, *Phys. Rev. E* **74**, 046101 (2006)
  - [11] T. Rohlf, N. Gulbahce and C. Teuscher, *Phys. Rev. Lett.* **99**, 248701 (2007)
  - [12] M. Leone et al., *J. Stat. Mech.* (2006) P12012
  - [13] R. Albert and H. G. Othmer, *J. Theor. Biol.* **223**, 1-18 (2003)
  - [14] S. Braunewell and S. Bornholdt, *J. Theor. Biol.* **245**, 638-643 (2007)
  - [15] P. Ramö, J. Kesseli and O. Yli-Harja, *J. Theor. Biol.* **242**, 164 (2006)
  - [16] T. Rohlf and S. Bornholdt, *JSTAT* L12001 (2005); T. Rohlf and S. Bornholdt, *q-bio.MN/0401024* (2004)
  - [17] E. R. Jackson et al., *J. Theor. Biol.* **119**, 379-396
  - [18] S. Bornholdt and T. Rohlf, *Phys. Rev. Lett.* **84** (2000) 6114
  - [19] S. Bornholdt and T. Röhl, *Phys. Rev. E* **67**, 066118 (2003)
  - [20] M. Liu and K.E. Bassler, *Phys. Rev. E* **74**, 041910 (2006)
  - [21] A. A. Moreira and L.A.N. Amaral, *Phys. Rev. Lett.* **94**, 218702 (2005)
  - [22] K.E. Kürten, *Phys. Lett. A* **129** (1988) 157-160.
  - [23] K.E. Kürten, *J. Phys. A* **21** (1988) L615-L619.
  - [24] T. Rohlf and S. Bornholdt, *Physica A* **310**, 245-259 (2002).
  - [25] I. Nakamura, *Eur. Phys. J. B.* **40**, 217-221 (2004)
  - [26] M. Aldana and H. Larralde, *Phys. Rev. E* **70**, 066130 (2004)
  - [27] M. Aldana, *Physica D*, **185(1)**, 45-66 (2003)
  - [28] F. Greil and B. Drossel, *arXiv:cond-mat/0701176v1*

(2007)

- [29] S. Patarnello and P. Carnevali, in: *Neural computing architectures - the design of brain-like machines*, ed. I. Aleksander, MIT Press, Cambridge, MA (1989)
- [30] N. Bertschinger and T. Natschläger, *Neural Computation* **16(7)**, 1413-1436 (2004)
- [31] A.F. Bompfünnewer et al., *Th.Biosci.* **123**, 301-369 (2005)
- [32] T. Rohlf, manuscript in preparation (2007)
- [33] P. Fronczak and A. Fronczak, arXiv:0712.0882 (2008)
- [34] We restrict ourselves to negative (or zero) thresholds, to ensure that the 'default state' of a network site  $i$ , i.e. when its inputs sum to zero, is to be 'inactive' ( $\sigma_i = -1$ ), which naturally excludes positive thresholds.
- [35] Other authors define  $\text{sgn}(0) = +1$ , however, for symmetry reasons update dynamics is not affected by either choice. If we interpret the state  $\sigma_i = -1$  as 'inactive' and, correspondingly,  $+1$  as 'active', our choice appears to be more natural: the default state of a network site is to be 'inactive', unless it receives activating inputs from other sites.
- [36] To obtain accurate results, one has to consider networks sizes  $N \gg \bar{K}$ , and adjust the upper limit of the sum in (10) accordingly. Since a small step size  $\Delta \bar{K}$  has to be applied iteratedly to identify  $K_c$ , this becomes computationally very costly.

## APPENDIX A: DERIVATION OF $p_s(k, |h|)$

In this section, we provide a derivation of the local damage propagation probability  $p_s(k, |h|)$ .

Consider a network site  $i$  with  $k$  inputs;  $k_+$  of these have positive sign,  $k_-$  negative sign, hence,  $k_+ + k_- = k$ . We now derive the conditions under which an inversion of one input spin at time  $t$  leads to a switch of the output of site  $i$  at time  $t + 1$ .

**1)  $k - |h|$  odd:** From Eqs. 1 and 2 it is easy to see that input-spin flips produce "damage" only if one of the following conditions holds:

$$k_+ - k_- - |h| = 1 \quad (\text{A1})$$

or

$$k_+ - k_- - |h| = -1. \quad (\text{A2})$$

In case A1, only the reversal of positive spins is effective, whereas in case A2, only the reversal of negative spins has an effect. We have

$$k_+ = \frac{k + |h| + 1}{2} \quad (\text{A3})$$

in the first case and

$$k_- = \frac{k - |h| + 1}{2} \quad (\text{A4})$$

in the second case. There is a total number of  $k \cdot 2^k$  possible spin configurations, of which  $\binom{k}{(k+|h|+1)/2}$  fulfill condition A3 and  $\binom{k}{(k-|h|+1)/2}$  fulfill condition A4.

Hence, the damage propagation probability follows as

$$p_s(k, |h|) = k^{-1} \cdot 2^{-(k+1)} \cdot \left[ (k + |h| + 1) \cdot \binom{k}{\frac{k+|h|+1}{2}} + (k - |h| + 1) \cdot \binom{k}{\frac{k-|h|+1}{2}} \right] \quad (\text{A5})$$

$$= \frac{2^{-(k-1)}(k-1)!}{[(k+|h|-1)/2]![(k-|h|-1)/2]!} \quad (\text{A6})$$

$$= 2^{-(k-1)} \binom{k-1}{\frac{k+|h|-1}{2}}. \quad (\text{A7})$$

**2)  $k - |h|$  even:** Here, we have as necessary conditions

$$k_+ - k_- - |h| = 0 \quad (\text{A8})$$

or

$$k_+ - k_- - |h| = 2. \quad (\text{A9})$$

In the first case, only the reversal of negative spins is effective, whereas in the latter case the same holds for positive spins. We have

$$k_- = \frac{k - |h|}{2} \quad (\text{A10})$$

in the first case and

$$k_+ = \frac{k + |h| + 2}{2} \quad (\text{A11})$$

in the second case. There is a total number of  $k \cdot 2^k$  possible spin configurations, of which  $\binom{k}{(k-|h|)/2}$  fulfill condition A10 and  $\binom{k}{(k+|h|+2)/2}$  fulfill condition A11. Hence, the damage propagation probability follows as

$$p_s(k, |h|) = k^{-1} \cdot 2^{-(k+1)} \cdot \left[ (k - |h|) \cdot \binom{k}{\frac{k-|h|}{2}} + (k + |h| + 2) \cdot \binom{k}{\frac{k+|h|+2}{2}} \right] \quad (\text{A12})$$

$$= \frac{2^{-(k-1)}(k-1)!}{[(k-|h|-2)/2]![(k+|h|)/2]!} \quad (\text{A13})$$

$$= 2^{-(k-1)} \binom{k-1}{\frac{k+|h|}{2}}. \quad (\text{A14})$$

## APPENDIX B: DERIVATION OF THE SCALING EQUATION

For RTN with Poisson distributed in- and out-degree, the critical line is given by the condition

$$\bar{d}(t+1) = \langle p_s \rangle (K_c(|h|), |h|) \cdot K_c(|h|) = 1. \quad (\text{B1})$$

with

$$\langle p_s \rangle (\bar{K}, |h|) = e^{-\bar{K}} \sum_{k=|h|}^{\bar{K}} \frac{\bar{K}^k}{k!} p_s(k+1, |h|). \quad (\text{B2})$$

Instead of averaging over the ensemble of all possible network topologies as in Eq. (B2), we now make an explicit *mean field approximation*, and consider a "typical" network node with  $k \approx \bar{K}$  inputs. Consequently, we approximate

$$\langle p_s \rangle(\bar{K}, |\bar{h}|) \approx p_s(\lfloor \bar{K} \rfloor, |h|), \quad (\text{B3})$$

where  $\lfloor \cdot \rfloor$  denotes the floor function. In the limit of large  $\bar{K}$  and  $|h|$ , the difference between the damage propagation probabilities for even and odd  $k$  vanishes, i.e. we can set

$$\langle p_s \rangle(\bar{K}, |\bar{h}|) \approx 2^{-\lfloor \bar{K} \rfloor - 1} \binom{\lfloor \bar{K} \rfloor - 1}{\frac{\lfloor \bar{K} \rfloor + |h|}{2}}, \quad (\text{B4})$$

and hence

$$\bar{d}(\bar{K}, |h|) = \bar{K} \cdot 2^{-\lfloor \bar{K} \rfloor} \binom{\lfloor \bar{K} \rfloor}{\frac{\lfloor \bar{K} \rfloor + |h|}{2}} \quad (\text{B5})$$

without loss of generality.

Using the Stirling approximation  $n! \approx n^n e^{-n} \sqrt{2\pi n}$ , dropping the floor function (since we now consider a function of real-valued variables only) and taking logarithms, we obtain

$$\ln [\bar{d}(\bar{K}, |h|)] \approx \ln \bar{K} - \ln 2 \cdot \bar{K} + Z_1 - Z_2 - Z_3 \quad (\text{B6})$$

with

$$Z_1 = \ln [\bar{K}^{\bar{K}} e^{-\bar{K}} \sqrt{2\pi \bar{K}}],$$

$$Z_2 = \ln \left[ \left( \frac{\bar{K} - |h|}{2} \right)^{\frac{\bar{K} - |h|}{2}} e^{-\frac{\bar{K} - |h|}{2}} \sqrt{\pi(\bar{K} - |h|)} \right]$$

and

$$Z_3 = \ln \left[ \left( \frac{\bar{K} + |h|}{2} \right)^{\frac{\bar{K} + |h|}{2}} e^{-\frac{\bar{K} + |h|}{2}} \sqrt{\pi(\bar{K} + |h|)} \right]$$

Summing out the logarithms in  $Z_1$ ,  $Z_2$  and  $Z_3$ , one realizes that all terms linear in  $\bar{K}$  drop out, resulting in

$$\begin{aligned} \ln [\bar{d}(\bar{K}, |h|)] &\approx \ln \bar{K} + \left( \bar{K} - \frac{1}{2} \right) \ln \bar{K} \\ &\quad - \frac{\bar{K} - |h| + 1}{2} \ln (\bar{K} - |h|) \\ &\quad - \frac{\bar{K} + |h| + 1}{2} \ln (\bar{K} + |h|) + C \end{aligned} \quad (\text{B7})$$

with  $C = \ln(\sqrt{2/\pi})$ . Using some simple algebra and approximating  $|h| + 1 \approx |h|$ , this can be reformulated as

$$\begin{aligned} \ln [\bar{d}(\bar{K}, |h|)] &\approx \ln \bar{K} - \frac{1}{2} \left\{ \ln \bar{K} \right. \\ &\quad \left. - \bar{K} \ln \left[ \frac{(\bar{K} + |h|)(\bar{K} - |h|)}{\bar{K}^2} \right] \right. \\ &\quad \left. + |h| \ln \left[ \frac{\bar{K} + |h|}{\bar{K} - |h|} \right] \right\} + C. \end{aligned} \quad (\text{B8})$$

This leads to the final result

$$\begin{aligned} \ln [\bar{d}(\bar{K}, |h|)] &\approx \frac{1}{2} \left\{ \ln \bar{K} - \bar{K} \cdot \ln \left[ 1 - \left( \frac{|h|}{\bar{K}} \right)^2 \right] \right. \\ &\quad \left. - |h| \ln \left[ \frac{\bar{K} + |h|}{\bar{K} - |h|} \right] \right\} + C. \end{aligned} \quad (\text{B9})$$

### APPENDIX C: ASYMPTOTIC SCALING OF $K_c$

Let us now derive the asymptotic scaling behavior of the critical connectivity  $K_c(|h|)$ . We start with the case of homogeneous thresholds, and then generalize to inhomogeneous thresholds.

First, we note that the right hand-side of Eq. (B5) has the form of a Binomial distribution

$$P(n, k) = \binom{n}{k} p^n q^{n-k} \quad (\text{C1})$$

with  $p = q = 1/2$ ,  $n = \lfloor \bar{K} \rfloor$  and  $k = (\lfloor \bar{K} \rfloor + |h|)/2$ , multiplied with a prefactor  $\bar{K}$ . In the limit  $\bar{K} \rightarrow \infty$  and  $|h| \rightarrow \infty$ , we can replace the Binomial distribution with a Gaussian and drop the floor function, i.e.

$$\bar{d}(\bar{K}, |h|) = \bar{K} \cdot C_n \exp \left[ -\frac{\left( \frac{\bar{K} + |h|}{2} - \frac{\bar{K}}{2} \right)^2}{2\bar{K} \cdot \frac{1}{2} \cdot \frac{1}{2}} \right]. \quad (\text{C2})$$

This simplifies to

$$\bar{d}(\bar{K}, |h|) = \bar{K} \cdot \sqrt{\frac{1}{2\pi\bar{K}}} \exp \left[ -\frac{\bar{h}^2}{2\bar{K}} \right] \quad (\text{C3})$$

with the normalization constant  $C_n = \sqrt{1/(2\pi\bar{K})}$  and variance  $\sigma^2 = \bar{K}$ .

In the case of inhomogeneous thresholds, we can still use this approximation, however, the variance  $\sigma_h^2$  of the threshold distribution adds to the variance of the damage propagation function of the homogeneous case. This implies that we have to replace  $\bar{K}$  with  $\bar{K} + \sigma_h^2$ , and hence

$$\bar{d}(\bar{K}, |h|) = \frac{\bar{K} + \sigma_h^2}{\sqrt{2\pi(\bar{K} + \sigma_h^2)}} \exp \left[ -\frac{\bar{h}^2}{2(\bar{K} + \sigma_h^2)} \right] \quad (\text{C4})$$

To obtain the criticality condition, we take logarithms and set the result to zero, leading to

$$\ln [K_c + \sigma_h^2] - \frac{1}{2} \ln [2\pi(K_c + \sigma_h^2)] - \frac{\bar{h}^2}{2(K_c + \sigma_h^2)} = 0. \quad (\text{C5})$$

This simplifies to

$$\bar{h}^2 = (K_c + \sigma_h^2) \ln \left[ \frac{K_c + \sigma_h^2}{2\pi} \right]. \quad (\text{C6})$$

To solve this equation with respect to  $K_c$ , we make the ansatz

$$K_c + \sigma_h^2 \approx \frac{\bar{h}^2}{2 \ln |\bar{h}|}. \quad (\text{C7})$$

Inserting for  $K_c + \sigma_h^2$  into Eq. (C6), we obtain

$$\bar{h}^2 \approx \frac{\bar{h}^2}{2 \ln |\bar{h}|} \ln \left[ \frac{\bar{h}^2}{4\pi \ln |\bar{h}|} \right] \quad (\text{C8})$$

$$= \bar{h}^2 \left\{ 1 - \frac{\ln [4\pi \ln |\bar{h}|]}{2 \ln |\bar{h}|} \right\}. \quad (\text{C9})$$

Since the second term in the bracket vanishes logarithmically for  $|\bar{h}| \rightarrow \infty$ , we have verified that Eq. (C7) yields the correct asymptotic scaling. Consequently, the asymptotic scaling of the critical line for large  $|\bar{h}|$  is given by

$$K_c(|\bar{h}|) \approx \frac{\bar{h}^2}{2 \ln |\bar{h}|} - \sigma_h^2. \quad (\text{C10})$$

However, notice that the convergence is very slow, as can be appreciated from the logarithmic finite-size term in Eq. (C9). In particular, we conclude that the asymptotic scaling for networks with homogeneous thresholds, i.e.  $|h| = \text{const.}$  and  $\sigma_h = 0$  is given by

$$K_c^{\text{hom}}(|h|) \approx \frac{h^2}{2 \ln |h|}. \quad (\text{C11})$$

Let us now prove that this scaling is universal for  $|\bar{h}| \rightarrow \infty$  for all threshold distributions possessing a variance  $\sigma_h^2 \sim |\bar{h}|^\alpha$  with  $0 \leq \alpha < 2$ . In this case, we have

$$\lim_{|\bar{h}| \rightarrow \infty} \frac{K_c(|\bar{h}|)}{K_c^{\text{hom}}(|\bar{h}|)} = \lim_{|h| \rightarrow \infty} \frac{K_c^{\text{hom}}(|h|) - \sigma_h^2}{K_c^{\text{hom}}(|h|)} \quad (\text{C12})$$

$$= 1 - \lim_{|h| \rightarrow \infty} \frac{\sigma_h^2}{K_c^{\text{hom}}(|h|)} \quad (\text{C13})$$

$$= 1 - \lim_{|h| \rightarrow \infty} \frac{2 \ln |h| \cdot |h|^\alpha}{h^2} \quad (\text{C14})$$

$$= 1 - \lim_{|h| \rightarrow \infty} \frac{2 \ln |h|}{|h|^{2-\alpha}}. \quad (\text{C15})$$

Since we assumed  $0 \leq \alpha < 2$ , the limit in Eq. (C15) vanishes, and hence the asymptotic scaling equation C11 is indeed universal for this class of threshold distributions.

#### APPENDIX D: ASYMPTOTIC SCALING OF $K_d$

The characteristic connectivity  $K_d$  is defined by the conditions:

$$|h| = |\bar{h}|, \quad (\text{D1})$$

where  $|h|$  is the (constant) threshold of a homogeneous network, and  $|\bar{h}|$  the average threshold of a corresponding network with inhomogeneous thresholds, and

$$\bar{d}^h(K_d(|h|), |h|) - \bar{d}^i(K_d(|h|), |\bar{h}|) = 0, \quad (\text{D2})$$

where  $\bar{d}^h$  is the expected damage for homogeneous networks, and  $\bar{d}^i$  is the expected damage for inhomogeneous

networks. Let us further assume that thresholds are Poissonian distributed, i.e.  $\sigma_h^2 = |h|$ . If we apply the same Gaussian approximation as in section C, these conditions lead to

$$\frac{e^{-h^2/(2K_d)}}{\sqrt{2\pi K_d}} = \frac{e^{-h^2/(2(K_d+|h|))}}{\sqrt{2\pi(K_d+|h|)}}. \quad (\text{D3})$$

Taking logarithms and reordering, this reduces to

$$\ln \left[ \frac{K_d + |h|}{K_d} \right] - \frac{h^2}{K_d} + \frac{h^2}{K_d + |h|} = 0 \quad (\text{D4})$$

Linearization of the first term leads to the approximation

$$\frac{|h|}{K_d} - \frac{h^2}{K_d} + \frac{h^2}{K_d + |h|} \approx 0. \quad (\text{D5})$$

Solving this equation for  $K_d$  finally yields the asymptotic scaling

$$K_d(|h|) \approx h^2 - |h|, \quad (\text{D6})$$

i.e.  $K_d$  scales quadratically with  $|h|$ .

#### APPENDIX E: POWER-LAW APPROXIMATION OF $K_c(|h|)$ FOR FINITE $|h|$

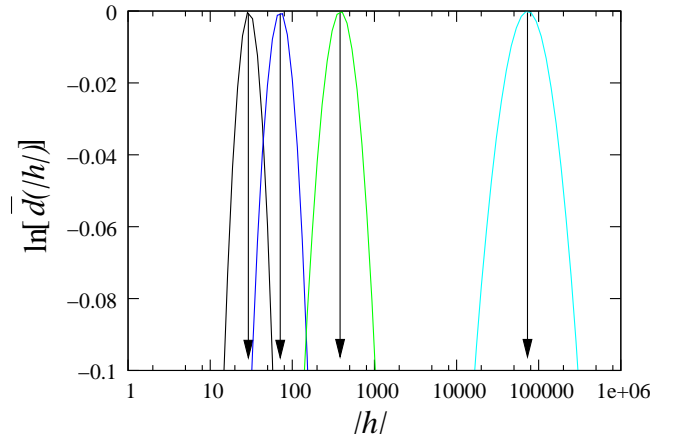


FIG. 18: Solutions of Eq. (E3) for (from the left to the right)  $\alpha = 1.6$ ,  $\alpha = 1.7$ ,  $\alpha = 1.8$  and  $\alpha = 1.9$ . Projections of the maximum on the  $|h|$ -axis (as indicated by arrows) yield the corresponding values of  $|h|_c$  at which the approximations are optimal.

In this section, we first describe how to identify numerically candidate solutions (power-laws)

$$K_c(|h|) \approx a(|h|) \cdot |h|^{\alpha(|h|)} \quad (\text{E1})$$

that optimally approximate Eq. (14) for finite (critical)  $|h|_c$ .

We start with a fixed  $\alpha \in [1.6, 2)$  and define

$$F(y) := \frac{1}{2} \left\{ \ln y - y \cdot \ln \left[ 1 - \left( \frac{|h|}{y} \right)^2 \right] - (|h| + 1) \ln \left[ \frac{y + |h|}{y - |h|} \right] \right\} + C \quad (\text{E2})$$

with  $y = a \cdot |h|^\alpha$ . One can show that, for any finite  $a$  and  $\alpha$ ,  $F(y)$  has a maximum at a finite value  $|h|_{max}$ . We know that  $K_c$  is a monotonically increasing function of  $|h|$ , and intend to optimize the power-law approximation exactly at  $K_c$ . Hence, we have to vary  $a$  such that

$$\max_a F(y)|_\alpha = 0. \quad (\text{E3})$$

Projection of the maximum on the  $|h|$ -axis then yields the corresponding threshold values  $|h|_c(\alpha)$  at which the approximation for the given  $\alpha$  is optimal (Fig. 18). Inversion of this relation allows us to plot the corresponding values of the function  $\alpha(|h|)$  (Fig. 8).

Last, let us estimate the asymptotic scaling of  $\alpha(|h|)$ . If we apply the asymptotic scaling relation for  $K_c$  derived

in section C, we can approximate

$$\frac{h^2}{2 \ln |h|} = a(|h|) \cdot |h|^{\alpha(|h|)}. \quad (\text{E4})$$

Taking logarithms, this yields

$$2 \ln |h| - \ln 2 - \ln \ln |h| = \ln a(|h|) + \alpha(|h|) \ln |h|. \quad (\text{E5})$$

We now consider variations of  $\alpha$  only, i.e. we fix  $a$  with respect to  $|h|$ . Taking the derivative with respect to  $|h|$  on both sides of the equation and solving for  $\alpha$  then yields

$$\alpha(|h|) \approx 2 - \frac{1}{\ln |h|}. \quad (\text{E6})$$

Inserting this result into Eq. (E5), we finally obtain the estimate

$$a(|h|) \approx \frac{e}{2 \ln |h|} \quad (\text{E7})$$

for the proportionality constant  $a$ .